RESEARCH ARTICLE OPEN ACCESS

Large Eddy Simulation of Turbulence Modeling for wind Flow past Wall Mounted Cubical Building Using Smagorinsky Scheme and validation using Artificial Neural Network for Time Series Data

Bibhab Kumar Lodh*, Ajoy K Das**, N. Singh***
*(Department of Chemical Engineering, National Institute of Technology Agartala, West Tripura-799046)
** (Department of Mechanical Engineering, National Institute of Technology Agartala, West Tripura-799046)
*** (Department of Aerospace Engineering, IIT Kharagpur, West Bengal)

ABSTRACT
This paper will present the large eddy simulation of turbulence modeling for wind flow over a wall mounted 3D cubical model. The LES Smagorinsky scheme is employed for the numerical simulation. The domain for this study is of the size of 60 cm x 30 cm x 30 cm. The 3D cube model is taken of the size of 6 cm x 6 cm x 4 cm. The Reynolds number for the flow in respect of the height of the cube i.e, 4 cm is $5.3x10^4$. The hexahedral grids are used for the meshing of the flow domain. The results are discussed in terms of various parameters such as velocity profile around the cube and the computational domain, the pressure distribution over the cube, near wall velocity profile and the shear stress distribution and also the result of drag coefficient is verified by neural network time series analysis using MATLAB. In this present study we have used the OpenFoam platform for the computational and numerical analysis. The numerical scheme employed is the combination of the steady state incompressible Newtonian flow model using SIMPLE algorithm followed by the transient model of incompressible Newtonian flow using PISO algorithm. We have observed that there is a constant positive drag coefficient in case of steady state simulation where as there is a negative lift coefficient in the initial run and a very low lift coefficient at the end of the steady state simulation.

Keywords **-** Large eddy simulation, Smagorinsky, Spalartallmaras DDES, 3D cubical model, SIMPLE algorithm, PISO algorithm, Reynolds no., OpenFoam, Artificial neural network

I. INTRODUCTION

Unsteady separated flows around a cube are very significant for many engineering problems. We have performed Large Eddy Simulation (LES) of three dimensional flow field around a wall mounted cube with sharp corners which is supposed to be a benchmark problem in turbulence modelling for flow over bluff bodies.

The aim of the present work is to find the results around three dimensional flow fields by using LES model such as: Smagorinsky Model [1]. Turbulent flows are significant in case of wind flow around bluff bodies such as building, towers etc and are highly affected by the solid walls around the body. The viscous affected regions are generally governed by the walls and have very large gradients and hence these regions should have accurate presentation for the true prediction of wall bounded flow[3]. Turbulence is an unpredictable state of fluid and is one of the most challenging problems in fluid dynamics. Turbulent flows incorporate a hierarchy of eddies or whirls which ranges from very large scale to very small scale in sizes. Energy is transferred between these scales are generally from larger to smaller scales until finally the smallest scales are dissipated into heat by molecular viscosity. This energy cascade theory was introduced into physical laws for the various scales present in turbulent flow by Russian Scientist Kolmogorov[4].

The study of turbulent flows can be divided in three main categories: Analytical theory, physical experiments and numerical simulation. Numerical simulation has become very popular in the last couple of decades since it is lot more flexible and cost effective than the real experimental method. Also due to the complexity of the flow behaviour it is not always possible to perform or visualize the experimental results due to lack of high precision equipment or due to the cost of those equipments. Computational methods have been applied in wind engineering to study wind flow pattern around buildings or a group of buildings with a view to understand flow interference effects and its relation to pollution dispersion, pedestrian comfort, ventilation in the building etc. Aerodynamic forces on the buildings have also been predicted through numerical simulation. The main complications of using numerical method arise due to bluff body shape of the structures with sharp corners in contrast with streamline bodies used in aerospace applications.

Complicated flow fields around buildings consisting of impingement, flow separation, streamline curvature, reattachment and vortex formation remains the most challenging problem for computational specialists to tackle. Further complications arise due to presence of turbulence. Anisotropic strain rates that develop on the body lead to complicated turbulence characteristics which have put a question mark on kind of modelling to be used for turbulence simulation.

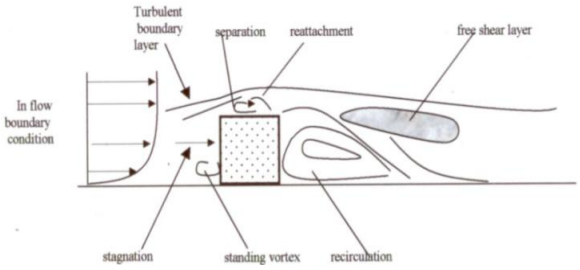

Fig. 1 Typical turbulent flow behaviour over a cubical body

The computational method has the advantage over the experimental work that any flow physical quantity can be measured at any point in the flow field and at any instance. One major drawback for the numerical simulation in case of engineering field is that the inability to give accurate result under any given condition and hence it is of utmost importance to validate the result of the simulation. The simulation of turbulent flow or the turbulence modelling has different approach and they can be named as: Reynolds Average Navier-Stokes (RANS), Large Eddy Simulation (LES), and Direct Numerical Simulation (DNS). The three above mentioned approaches can be represented in the figure below:

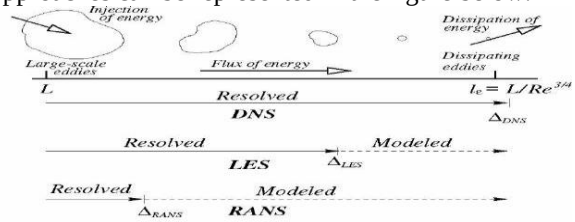

Fig. 2 Comparison between RANS, DNS and LES

The Reynolds Average Navier-Stokes (RANS) is generally used Applications that only require average statistics of the flow. It Integrate merely the ensemble-averaged equations and Parameterize turbulence over the whole eddy spectrum. The advantages of RANS are that it is computationally inexpensive, fast. Whereas the disadvantages are in this turbulent fluctuation not explicitly captured and also pparameterizations are very sensitive to large-eddy structure that depends on environmental conditions such as geometry and stratification Parameterizations are not valid for a wide range of different flows and hence it is not suitable for detailed turbulence studies. Direct Numerical Simulation (DNS) is the most straight-forward approach. It resolves all scales of turbulent flow explicitly. The advantage is that in principle it gives very accurate representation of flow field. The disadvantage is that it requires high level of computational resources. Hence DNS is restricted to moderately turbulent flow and highly turbulent flows cannot be simulated because of excessive time consumption and cost. The approach what we have implemented in this present study is the Large Eddy Simulation (LES) because of its advantages over the other two approaches of turbulence modelling. It seems to combine advantages and avoid disadvantages of DNS and RANS by treating large scales and small scales separately, based on Kolmogorov's theory of turbulence. The large eddies are explicitly resolved and the impact of small eddies on the large-scale flow is parameterized. The advantage of this method is that hhighly turbulent flows can be simulated. LES does not resolve the full range of turbulent scales (as DNS does), but it captures a much larger range of scales than the Reynolds average equations. Direct simulation is applied to the large scales, while the small scales are averaged out and their effects are modelled. This approach appears to be Justified because the large eddies contain most of the energy, do most of the transporting of conserved properties and vary most from case to case. In contrast, the smaller eddies are believed to be more universal (largely independent of the boundary conditions) and therefore easier to model. Since the contribution of the small-scale turbulence to the resolved flow field is small, the errors introduce by their modelling should also be small. In addition, the resolved scales carry much more information than the mean flow predicted by the RANS approach. LES is therefore potentially much more accurate than RANS and when compared to DNS, its demand on computer resources is considerably smaller, since the smallest scales need not be resolved. In addition, LES surface time-pressure histories have proven to be ideal for predicting low Mach number aero-acoustic noise sources, an important consideration in automotive design and other fields. Given all these factors, the steady increase in computing resources and the advancing development of the technique, LES promises to take a prominent role in design environments of the near future. From the above comparison it is very much clear that the LES modelling is much more suitable for high turbulence and hence we have implemented the LES subgrid model which is supposed to be one of the most suitable turbulence modelling tools. The details of the subgrid model will be discussed in the Numerical Approach section.

II. MODEL DESCRIPTION

Schematic representation of the flow field is given below:

Fig. 3 Domain Representation

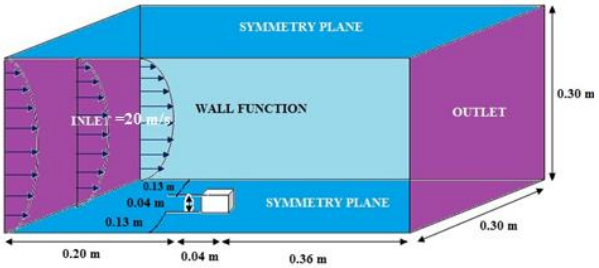

As represented in the figure, the cube is taken as side is of 0.04m. The domain length is 0.6 m, the width is 0.3m and the height is also 0.3m. The cube is placed at 0.2 m away from the inlet in X direction, 0.13 m away from the front and back panel in Z direction and at zero meter i.e., at the face of the lower wall symmetry plane in Y direction. The inlet wind velocity is taken as (20, 0, 0) i.e. 20 m/s in horizontal direction and is considered as the inlet as fully developed flow condition. The upper and lower walls are taken as symmetry plane where as the front and back panel of the flow field is taken as nutuspaldingwall function and also the walls of the cube are also considered to be the same wall function. The pressure at the walls is taken as zero gradients where as the velocity components are taken as zero at all wall faces. The internal flow field is considered to be the same as the inlet velocity condition i.e., (20, 0, 0). The turbulent k is considered to be 0.24 initially, turbulent omega is considered as 1.78 and the pressure is taken as zero at initial. The domain coordinates ranges are (-0.2 to 0.4), (0 to 0.3) and (-0.13 to 0.17).

III. NUMERICAL APPROACH

In this present study two simultaneous solvers in OpenFoam platform were applied for both the cases as mentioned above. It is already been established in CFD forum that OpenFoam is supposed to be one of the strongest tool for CFD modelling. This is a very well known fact that it is very difficult to predict and implement the initial boundary condition in case of LES modelling and hence at the first stage of simulation a steady state solver is used using simpleFoam which runs on SIMPLE algorithm[5] and the result or the steady state value has been taken as initial case for the implementation of the unsteady state by using pisoFoam which runs on PISO algorithm[6]. Before the description of the solvers we must first look at the meshing of the domain which is supposed to be the heart of any CFD simulation. The work was performed under Linux OS in Ubuntu 12.10 and with OpenFoam 2.3.0.

A. Mesh Generation

In our present studies the blockMesh facility of the openFoam was used to mesh the domain of fig.3. The domain has been meshed by using hexahedra mesh with 2000 cells (20x10x10). The cubical body has been generated in FreeCad and is exported as a .stl format in openFoam. After the importing of the cube geometry by using the snappyHexMesh utility of the openFoam the mesh of the whole geometry and the domain were refined in three stages as per the requirement. OpenFoam gives the flexibility to check the criteria for the good meshing using checkMesh utility and it is found that the mesh has been generated are acceptable as per the convention and the particulars of the mesh are given below as tabular form

Col 1	Col 2	Col 3	Col 4	Col 5	Col 6
Time	Faces	Internal faces	Cells	Hexahedra	Prism
0	6500	5500	2000	2000	-
1	2065098	2010555	672791	658418	-
2	2064214	2010555	672791	657834	568
3	2112255	2058194	688611	672914	568

Col 7	Col 8	Col 9	Col 10	Col 11	Col 12
Polyhedra	Max. Aspect ratio	Min. Vol.	Max. Vol.	Total Vol.	Max skewness
-	1	2.7×10^{-5}	2.7×10^{-5}	0.054	9.25926×10^{-11}
14373	1.00032	1.03×10^{-10}	2.7×10^{-5}	0.054	1.00021
14389	3.00196	4.83×10^{-11}	2.7×10^{-5}	0.054	0.568001
15129	6.05776	1.997×10^{-11}	2.62×10^{-05}	0.054	1.91523

Table 1 Meshes generated at four stages and the parameter details

The final mesh of the whole geometry and the cube is shown below:

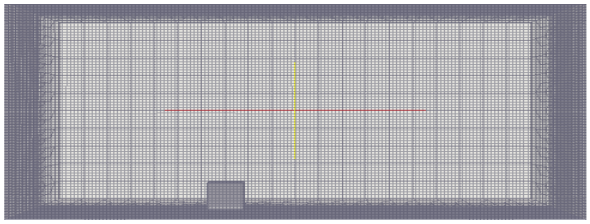

Fig. 4 Mesh of the whole domain with the cubical geometry after final stage of refinement

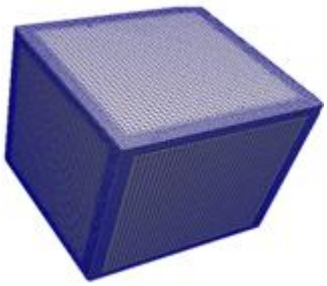

Fig. 5 Mesh of the cubical geometry after final stage of refinement

B. Steady State Solver

The simpleFoam as steady state solver was implemented. The OpenFoam uses finite volume scheme. The RAS model is incorporated with Spalartallmaras turbulence model. The classical averaging method is the ensemble average, which produces the Reynolds Average Navier-Stokes equations (RANS). From a practical point of view, this is equivalent to an infinite set of experiments being sampled at the same time, the average of all the flow fields representing the ensemble average. For a time independent and/or non-cyclic flow, ensemble averaging will produce the same result as time averaging. The RANS equations for an incompressible turbulent velocity field are given by:

$$\frac{\partial U}{\partial t}+\nabla.(UU)=-\frac{1}{\rho}\nabla P+\nabla.[\upsilon(\nabla U+(\nabla U)^T)]-\frac{1}{\rho}\nabla.\tau \quad (1)$$

where uppercase denotes averaged quantities. The averaging of the non-linear terms introduces new unknowns into the equation in the form of the Reynolds stress tensor, τ . This stress tensor represents the effects of all turbulent fluctuations and has to be modelled to close the system. A large number of turbulence models are available, from simple algebraic[7] to the commonly used $K-\varepsilon$ models[8], to full Reynolds stress closures[9].

C. Spalart Allmaras Turbulence Model

The DES technique, proposed by Spalart et al. (1997), is based on the SA eddy viscosity model (Spalart and Allmaras, 1994), which solves a single transport equation for a working variable $\tilde{\upsilon}$ that is related to the turbulent viscosity υ_t . This model includes a wall destruction term, which reduces the turbulent viscosity in the logarithmic layer and laminar sub layer, as well as transition terms, which provide a smooth transition from laminar to turbulent flow (Spalart and Allmaras, 1994). After neglecting the transition terms, the governing equation can be generated[10] .

The simpleFoam solver ran for incompressible flow taken as the kinematic viscosity of air as $1.5\text{x}10^{-5}$ and using Splartallmaras turbulence model for time=500 and delta T=1. Gauss linear upwind approach is used for finding divergence (U), divergence (k) and also for divergence (omega). The results will be discussed in the result and discussion section.

D. Transient Solver

The main part of this simulation lies on the study of flow field and the physical quantities in unsteady state. For unsteady state we have implemented subgrid scale LES models i.e. Smagorinsky. In this case we have used the pisoFoam by imparting the initial case from the steady state solver.

E. Concept of subgrid model of large eddy simulation

In LES the contribution of the large scale structures to momentum and energy transfer is computed exactly and the effect of the smallest scales of turbulence is modelled. Since the small scales are more homogeneous and universal and less affected by the boundary conditions than the large eddies the modelling effort is less and presumably more accurate. A filter operation is used to filter to filter the large scales.

F. Smagorinsky model

The standard subgrid scale model is Smagorinsky (1963) model. If the filter applied to the Navier Stokes equations, subgrid scale stresses will assume to be:

$$\tau_{\bar{ij}}=(\overline{\bar{u}_i\bar{u}_j}-\overline{u_i}\,\overline{u_j})+(\overline{\bar{u}_i\dot{u}_j}+\overline{\dot{u}_i\bar{u}_j}-\overline{\dot{u}_i\dot{u}_j}) \quad (2)$$

Where the over bars represents the filter operators. These stresses are similar to the classical Reynolds' stresses but differ in that they are consequences of special averaging and go to zero if the filter width goes to zero. The most commonly used subgrid scale model which correlates τ_{ij} to the large scale strain rate tensor is:

$$\tau_{ij}=-2\upsilon_T\overline{S_{ij}}+\frac{\delta_{ij}}{3}\tau_{kk} \quad (3)$$

where

$$\tau_{kk}=\overline{u'_k u'_k} \quad \text{and} \quad \overline{S_{ij}}=\frac{1}{2}\left(\frac{\partial\overline{u_i}}{\partial x_j}+\frac{\partial\overline{u_j}}{\partial x_i}\right)$$

After substituting equation (2) and equation (3) in filtered Navier-Stokes equation and performing non dimensionalization with respect to Ur and a specified characteristic length we get the required equation for calculating the provisional velocity field using a second order time accurate explicit Adams-Bashforth differencing scheme for the subgrid scale and diffusion terms.

G. Validation of Drag Coefficient by using time series tool in MATLAB

After the numerical computation and finding the drag force by using OpenFoam solver we have validated the drag force calculation by using the Neural Network Time series Tool of MATLAB by finding the regression analysis of the same and the results are listed in section IV.

IV. RESULTS & DISCUSSION

In this section the various parameters will be described in details by the two said large eddy simulation model. The vertical velocity profile of the X-Component of velocity (Ux) is mentioned here under at certain points in the X-direction throughout the vertical Y-direction of the domain at the end time of the simulation that is 500.1 for the two les models. The vertical velocity profile of Ux at X= -0.1, 0.02, 0.2 and while Y ranges from 0 to 0.3 and z 0.02 i.e. at the centre of the cube are shown below. The profiles are compared as:

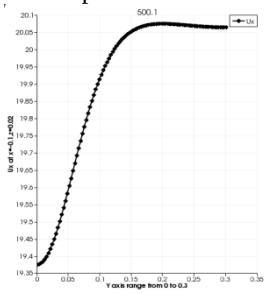

Fig. 6 Ux at X= -0.1 and Y= 0 to 0.3

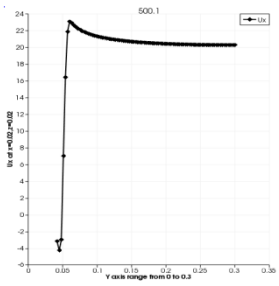

Fig. 7 Ux at X= 0. 02 and Y= 0 to 0.3

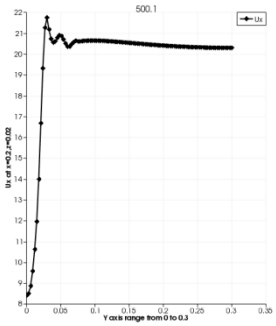

Fig. 8 Ux at X= 0. 2 and Y= 0 to 0.3

Fig. No 6,7,8 represents the said velocity profile for the Smagorinsky model. X= -0.1 represents the profile before the cube, X=0.02 represents the centre of the cube in X-direction where as X=0.2 represents the profile after the cube. In case of Smagorinsky at the centre of the cube the velocity reaches at maximum level and it deeps instantly giving a sharp decrease. In Smagorinsky the affect of cube at the exit region is quite high and hence we see a disturbed profile after the cube region. The velocity contour plot for both the cases at XY plane are shown below:

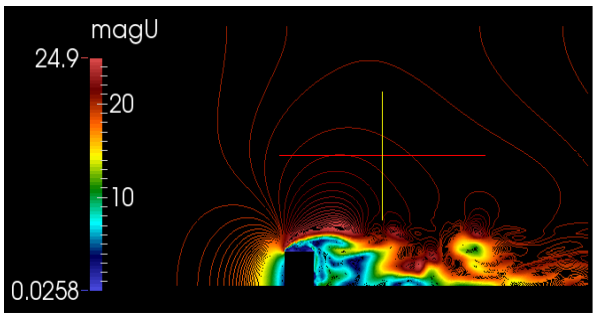

Fig.9 Velocity Contour at time 500.1 for Smagorinsky

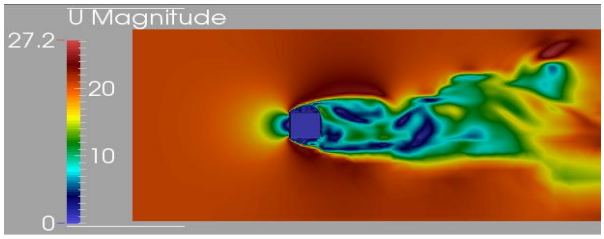

Fig.10 Velocity profiler at time 500.1 for Smagorinsky

It is clearly seen from the above figures that in case of fig 9. The velocity profile is much more chaotic even at the exit region and a lot of turbulence effect is there. The pressure distribution over the cube is of one of the main goal to find in this work. Since front face of the cube will be exposed to the wind hugely and hence we have found out the pressure distribution in the front face as well as in the top face of the cube and the results are as below:

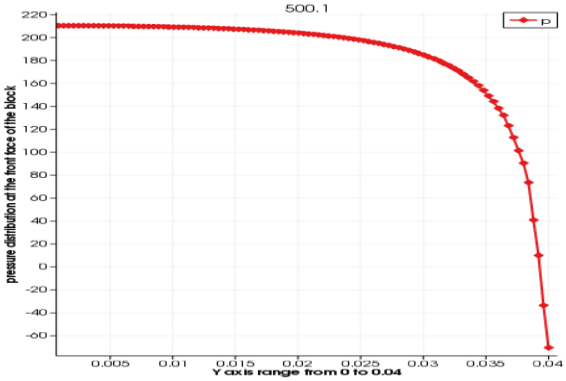

Fig. 11 Pressure at front face at the centre line of cube in Y-direction

It can be seen from the above fig there is a huge positive pressure developed in the front face of the cube. The maximum pressure is at the bottom of the cube and after the middle of the cube the pressure gradually decreases but in case of Smagorinsky model in fig. No. 11 the decrease is much smoother and the gradient is lower. It is also found that the pressure profile at the top face of the cube and is as follows:

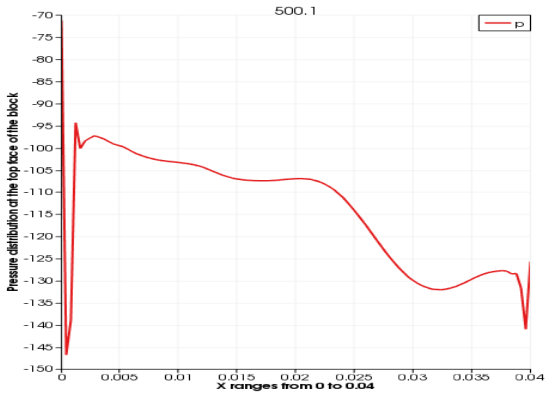

Fig. 12 Pressure at top face at the centre line of cube X-direction

The above plot shows the pressure distribution on the top face of the block through the centre line in X-direction. In the plot it is very clear that there is a negative pressure zone at the top of the cube. In the Fig. No. 12 it is seen though there is a negative pressure throughout as we progress from the entrance of the cube to the exit of the cube we see there is a decrease in pressure and also it is more disturbed since Smagorinsky model introduces lot more turbulence.

The pressure contours at XY plane are given below:

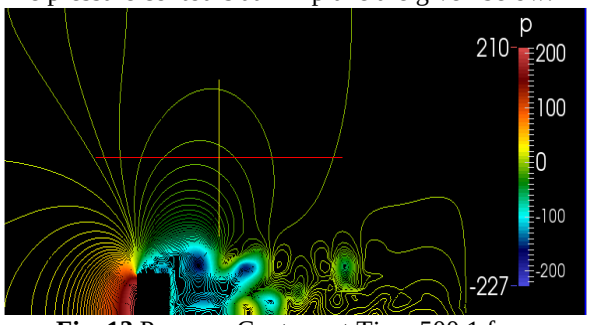

Fig. 13 Pressure Contour at Time 500.1 for Smagorinsky

From the above figure it is very much clear that just behind the cube there is much more circulating region in case of Smagorinsky model. From the colour bar it can be mention that the maximum pressure for Smagorinsky model is 210 and it shows the maximum pressure falls at the front face of the cube and at the top face there is negative pressure which can be verified from the pressure profile of fig no. 11, 12.

As already have mentioned that the data were written at every 100 time interval and hence some suitable interval is chosen so that it can be represented by the streamline flow over the cube to explain the flow behaviour for the full range of time from 500 to 500.1. For analysis the time is taken as 500, 500.003, 500.05 and 500.1. The streamlines are as follows:

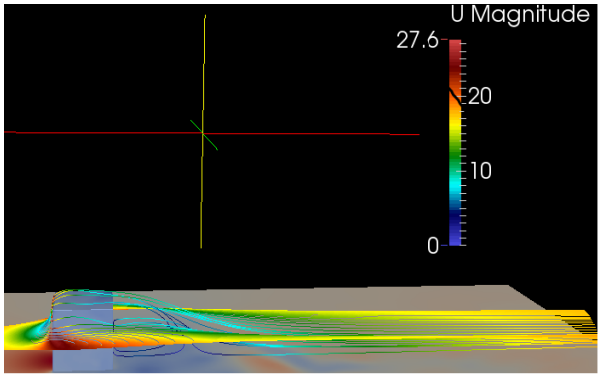

Fig. 14 The stream line profile for the Smagorinsky model at time=500, i.e. the end result of steady state solver

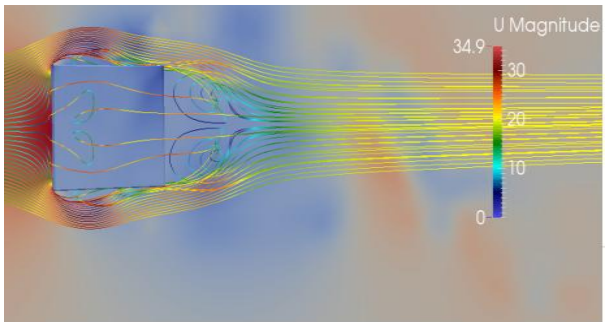

Fig. 15 Streamline at Time 500.003, Smagorinsky

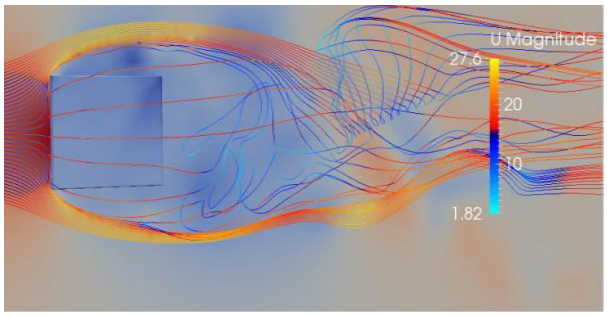

Fig. 16 Streamline at Time 500.05, Smagorinsky

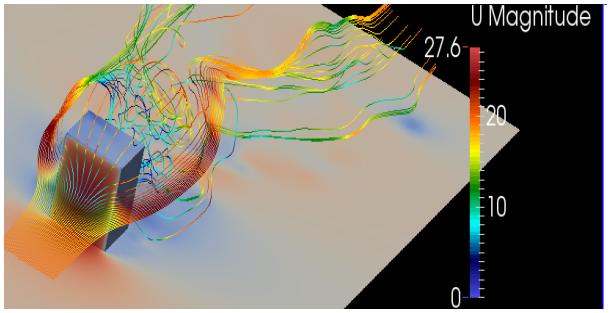

Fig. 17 Streamline at Time 500.1, Smagorinsky

Let us now describe the behaviour of streamline. In case of fig. No. 14 it can be seen that just adjacent to the back of the cube there is two symmetric vortex formation and after that it is a constant stream line since this is the outcome of the steady state solver. The two vortexes that have been formed are almost

half of the height of the cube. In fig. No. 15 which is the outcome of time 500.003 of the unsteady solver we see that flow has just started to separate at the top of the cube and also by two sides and there are formation of vortexes at the behind of the cube. In the midway of the total solver time that is in fig no. 16 at time 500.05 we can see the flow has become fully chaotic and total separation has been occur and the vortexes has been disappeared in the main stream of the flow in terms of energy cascading and the same thing has happened at the end of the simulation i.e. at time 500.1 represented by fig no.17.

Let us see the wall shear stress profile at the top face of the cube:

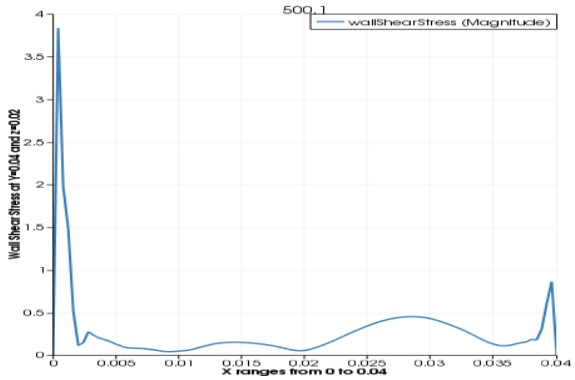

Fig. 18 Wall shear stress at the upper cube faces (Smagorinsky)

In case of Smagorinsky model in fig no 18 the maximum wall shear stress occurs just at the top of the start of the cube and value is near about 3.75. The behaviour is again with the same trend as we progress in X-direction there is lot more variation for Smagorinsky model. The Drag (C_D) and lift (C_L) coefficient in steady state and also in case unsteady transient les model were calculated. The results will be shown in terms of plots and they are as follows:

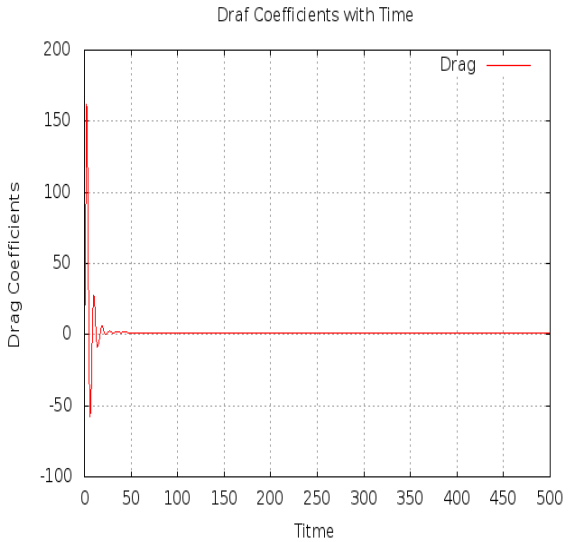

Fig. 19 Drag coefficient with time for steady state solver

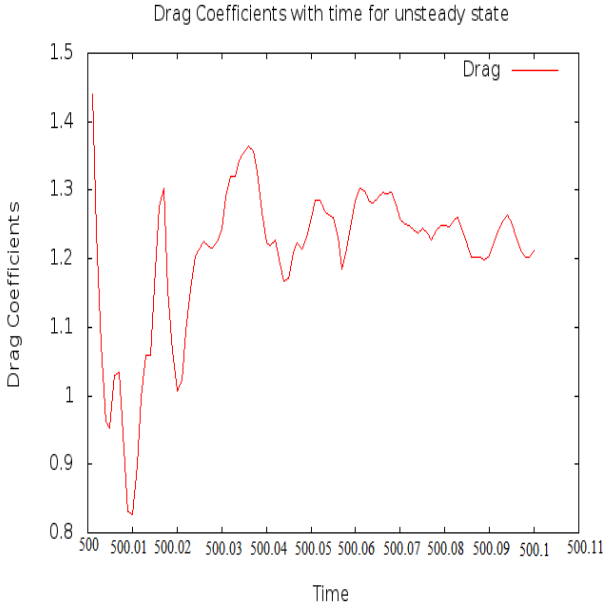

Fig. 20 Drag coefficient with time for unsteady solver for Smagorinsky

From the above plot no. 19 it is very much clear that since this is the outcome of the steady state solver hence we have got the straight line after initial time where there is certain variation. In this plot we have got the drag coefficient is very close to zero. Since the scale is quite high we have not got the actual drag but it is very clear that the drag coefficient is very close to zero.

Fig no. 20 shows the variation of Drag coefficient in case Smagorinsky model. It can be seen that there is a fluctuation in case of drag coefficient. The fluctuation is very rigorous initially but as the solver progress the magnitude of fluctuation diminishes and at the end of the solver we see there is very less fluctuation and hence we can say the solver has very close to convergence and if we run the system for more time we would actually reach to the point of convergence. The drag coefficient C_D is almost 1.2 from the plot. The Lift coefficient (C_L) is as follows:

In case of lift coefficient it is very obvious that the magnitude of C_L will have lesser value than that of C_D, in the plots below it shows that the maximum lift coefficient at any stage for Smagorinsky model is 0.3. The plot is of sinusoidal behaviour throughout and that shows that the lift coefficient does not have any stable throughout the solver time.

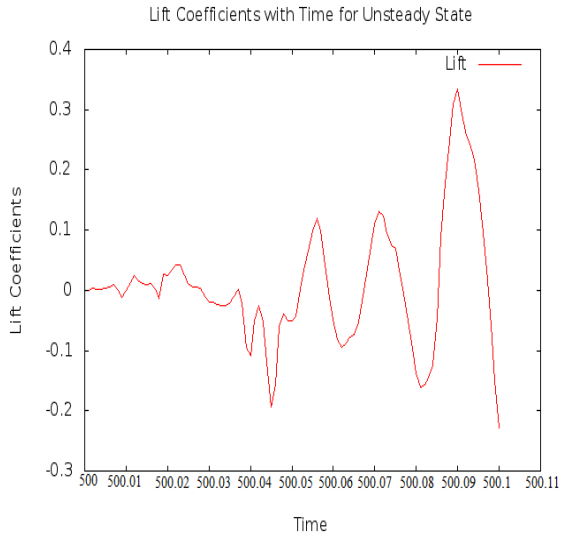

Fig. 21 Lift coefficient with time for unsteady solver for Smagorinsky

In case of any computational fluid dynamics (CFD) simulation one of the main considerations is the stability of the solver. To achieve temporal accuracy and numerical stability when running solver in OpenFoam a Courant number of less than 1 is required. The Courant number is defined for one cell as [12]:

$$Co = \frac{\delta t |U|}{\delta x} \tag{4}$$

Where δt is the time step, $|U|$ is the magnitude of the velocity through that cell and δx is the cell size in the direction of the velocity. The flow velocity varies across the domain and we must ensure Co<1 everywhere. So in order to keep Co below 1 we have to make the delta T in the solver in such a manner that the Courant no comes below 1 and hence we have chosen delta T as $10^{(-5)}$ and we got the Co in every iteration below 1 and which suggest the stability of our solver.

In case of validation of our solver and the result we got we choose to verify the Strouhal Number which is one of the benchmark and it is suggested that the Strouhal No should be less than 0.2. Strouhal No can be described as:

$$S_t = (f\ D/U) \tag{5}$$

Where f= Frequency for vortex Shedding, D= Diameter or the length scale, U=Bulk fluid velocity.

In search of finding the vortex shedding frequency the Fast Fourier Transformation of the time domain data of lift coefficient is used in Matlab and the fft plot for both the models are shown below:

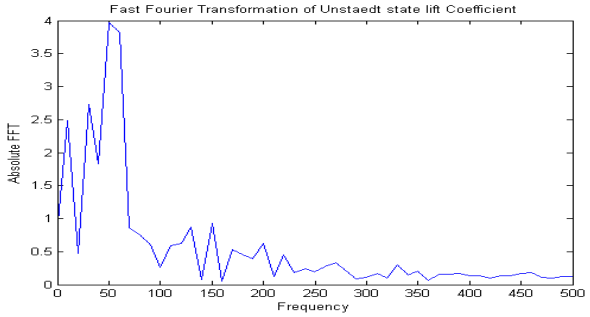

Fig. 22 FFT for lift Coefficient for Smagorinsky

From the above plot no. 22 it is seen that the maximum magnitude is for the frequency of 50. Hence we can take the vortex shedding frequency is f=50. Hence S_t= (50*0.04)/20=0.1.

In case of validation our results are compared with the experimental study carried out by Martinuzzi and Tropea[13] at Reynolds No. = 40, 000 in LES and also a series of works were published by Meinders and co-authors[14]-[17]. They showed that the flow separates at the top wall of the cube and there is secondary vortex at the rear corner of the cube whereas the main vortex occurs at the back of the cube. They also shown that there are four separate regions in the flow regime. The outcome of time-averaged streamlines obtained by Martinuzzi and Tropea at a high Reynolds number 40000 is shown in Fig. 23[13]. In the same contrast we also put our Smagorinsky model with Reynolds No. 53000 in fig. No. 24 to show the similarity between the two results.

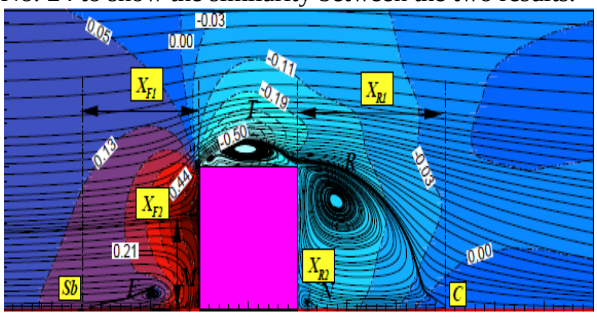

Fig. 23 Time-averaged streamlines for Reynolds No 40000[13]

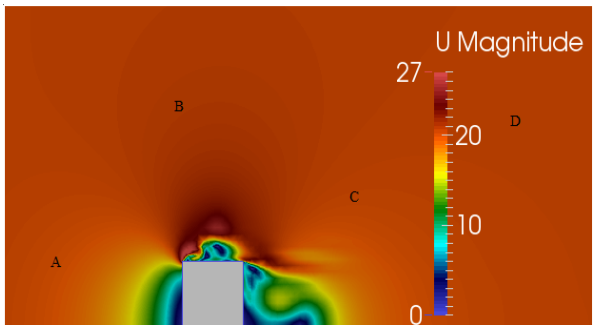

Fig. 24 Velocity profile for Reynolds No 53000

From the comparison of the two above figures we can see that in fig No. 23 there are four different regions and also in our simulation in fig No. 24 four regions as A, B, C & D are marked which shows that our results are very close to the published one. Several vortexes are observed, one at the roof, and one at the adjacent rear side of the cube and a small vortex at rear bottom corner of the cube. In our case it can be seen also there is vortex at the roof, a large vortex adjacent to the cube and also a small circulating zone at the rear bottom corner. There is some difference because of the difference of Reynolds no but the overall flow pattern is same.

As mentioned that the Strouhal Number = 0.1 in our present work, Alexander Yakhot , Heping Liu , Nikolay Nikitin have published a their result at 2006[18] and they showed that the Strouhal no for flow over cube at Reynolds number 5610 is 0.104. Thorsten Stoesser , Fabrice Mathey , Jochen Fröhlich , Wolfgang Rodi have worked on "les of flow over multiple cubes" and they have published their result on 2003[19] and they have reported the Strouhal no of 0.11 for Reynolds no 13000 which also very close to our result. Slight variation may occur due to difference in Reynolds no and also for the difference in boundary condition and the running of steady state simulation before the transient LES solver. In their work they have shown the surface streamline for the time averaged flow for multiple cubes are of the shape shown in fig no. 25. Whereas our time averaged velocity profile are also of the same shape as horse-shoe type vortex formation at the rear end of the cube shown in fig no. 26.

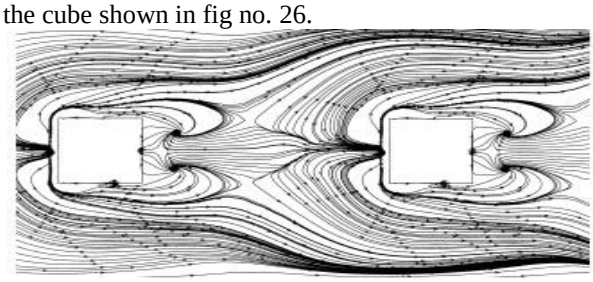

Fig. 25. Surface streamline for the time averaged flow for multiple cubes

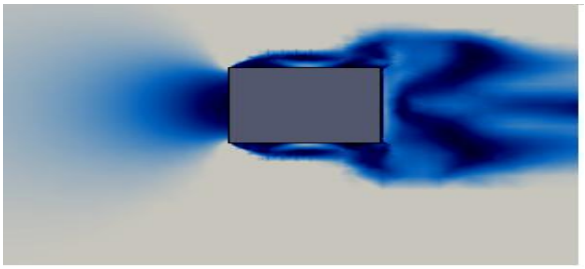

Fig. 26 Time averaged velocity profile showing horse shoe like complex behaviour for Smagorinsky

From the above two figure it is very much clear that both the profiles are almost same for the first cube which shows that our results are comparable with the published result.

The part of the above discussions were produced in the 30th National Convention and National Seminar on "Recent Trends in Research, Development and Innovation in Chemical Industries" on the paper "Numerical Comparison Of Large Eddy Simulation Of Turbulence Modeling For Flow Past Wall Mounted Cubical Building Using Smagorinsky and Spalartallmarasddes Scheme" by Bibhab Kumar Lodh, Ajoy K Das & N. Singh [21] and after that the below part is been added in this research article:

A. Validation of Drag Coefficient using Artificial Neural Network

At first we have trained our data by using nonlinear Autoregressive with external (Exogenous) input (NARX) which Predict series **y(t)** given **d** past values of **y(t)** and another series **x(t)**. Out of total data 70% data were taken for training the network, 15% were taken for validation and rest 15% were taken for testing. Number of hidden neurons were taken as 10 where as delayed were taken as 1.

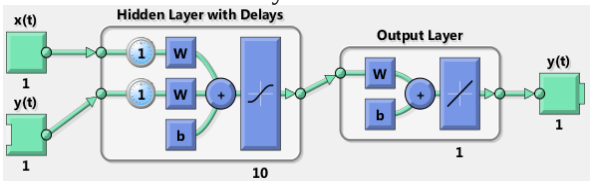

Fig. 27 Neural Network using 10 Neurons and delay 1

Then the network was trained and the corresponding simulink model is generated as :

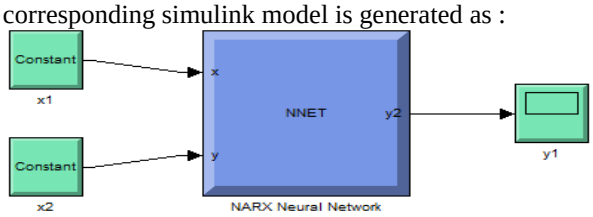

Fig. 28 Simulink model for corresponding neural network.

After the network is trained validation performance is shown below :

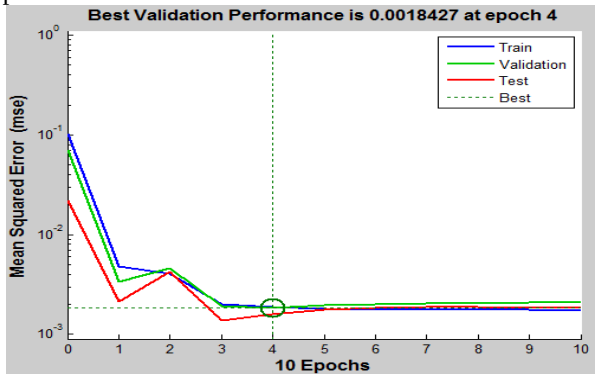

Fig. 29 validation performance for neural network

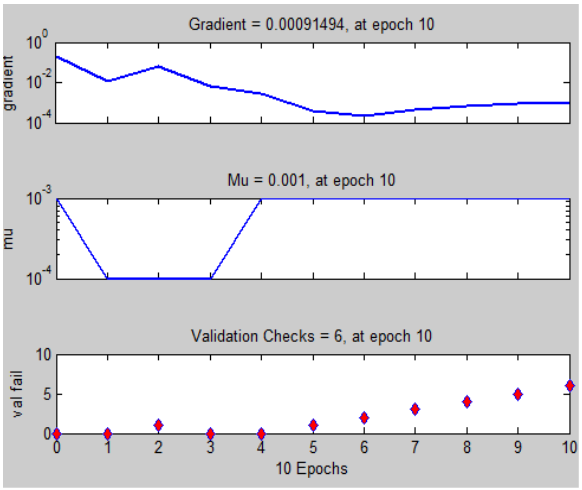

Fig. 30 Neural network training state at epoch 10

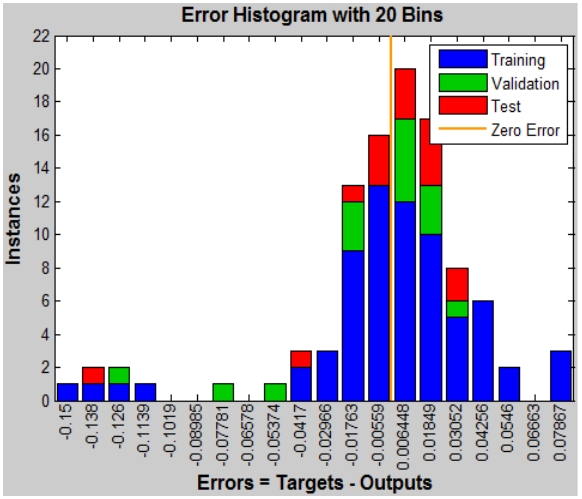

Fig. 31 The error histogram with 20 bins

The above graphs shows the errors between targets and output.

The regression graphs are shown separately for Training validation test and combined below:

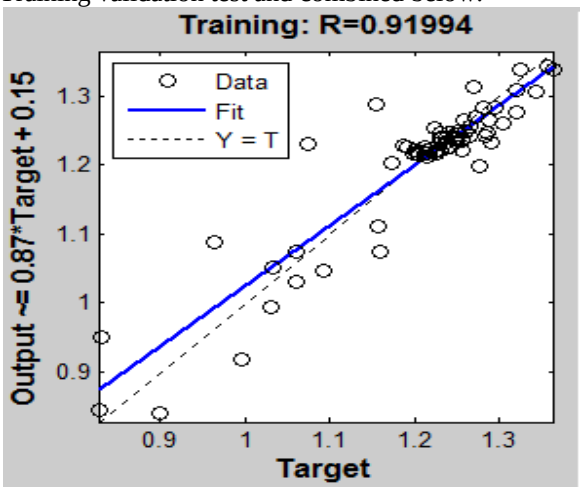

Fig. 32 Regression for training

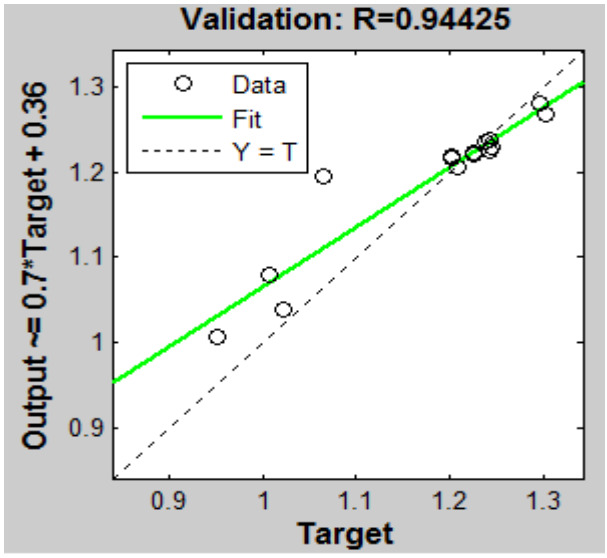

Fig. 33 Regression for validation

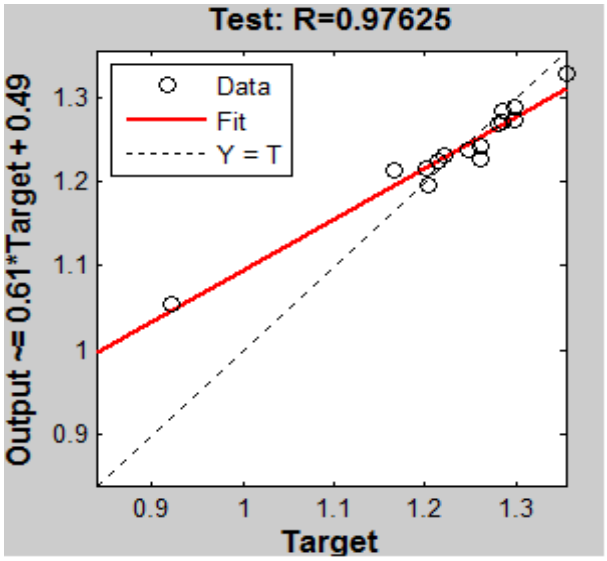

Fig. 34 Regression for Test

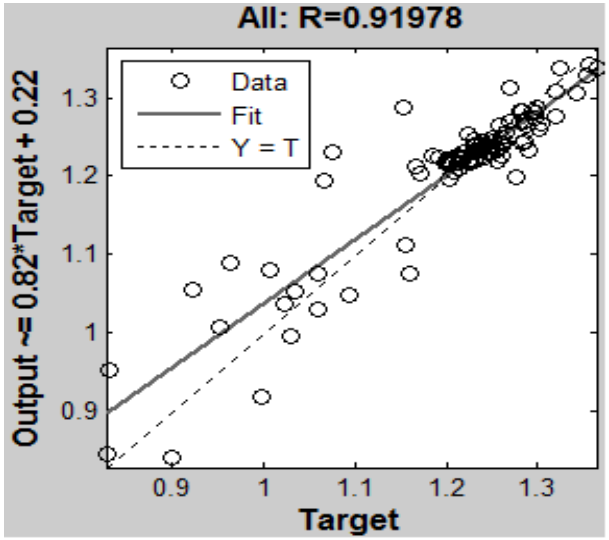

Fig. 35 Regression for all combined

From the above figures 32,33,34 & 35 we can see that all R value are above 0.91 which may be little bit on lower side but since this is the outcome of the numerical simulation result and the ANN and hence little lower value may be accepted.

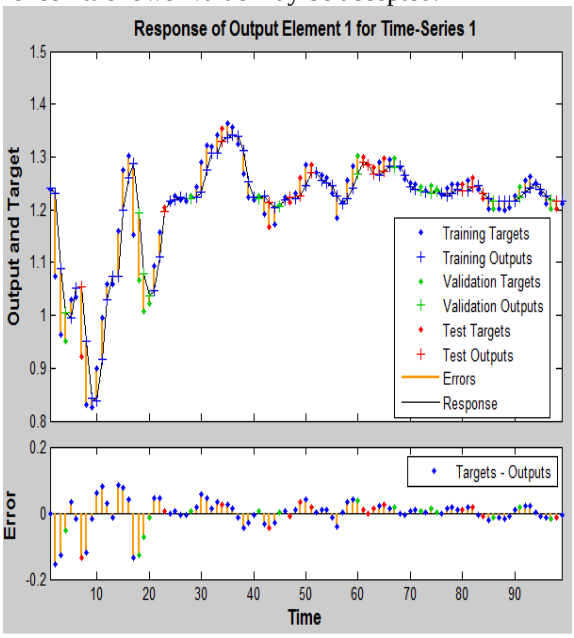

Fig. 36 Time series plot for network

From the above plot it can be seen that training targets (Blue dots) and the training outputs (blue plus) are almost at the same positions and which can be seen from the error plot below that all the values of (target-outputs) are lying within the limits which confirms the validation of the drag coefficients.

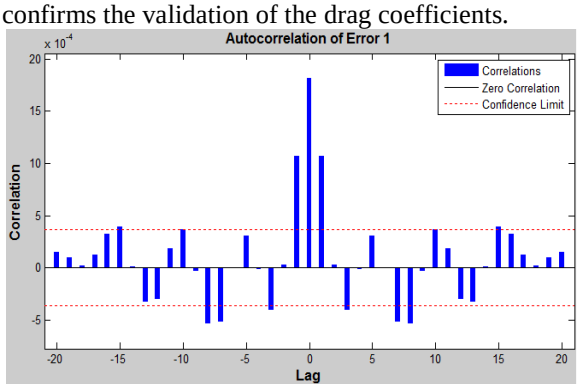

Fig. 37 Autocorrelation plot

From the above plot we can see that almost all the values are lying within the confidence limit in either half where as the ranges are very small and in the order of $10^{(-4)}$. It is very clear from the plot that that 86% of the correlated values are lying within the acceptable limit.

V. CONCLUSIONS

Large eddy simulation were performed using Smagorinsky for flow over a wall mounted cube using PISO algorithm for Reynolds number of 53000. We have considered fully developed flow. At first we have employed steady state simulation using SIMPLE algorithm so that we could use the steady state result for the initial condition for the large eddy simulation. We have presented our various results like velocity distribution, velocity profile, and pressure distribution over the front and the top face of the cube. We have also shown the variation of wall shear stress over the top face of the cube through the centre line. We have found some interesting characteristic regarding the flow field like the initial drag coefficient is very high and as the time progress the drag coefficient tries to reach a steady state value while the lift coefficient over the cube is never attained steady state and they show sinusoidal behaviour. We have also found the Strouhal no by finding the maximum frequency for vortex shedding for Karman Vortex Street and found that the Strouhal no is with accordance with other results published. We also shown that the horse-shoe type vortex in the adjacent rear face of the cube which is also been validated. Overall we can conclude that the Large eddy simulation proves to be a suitable alternative to direct numerical simulation (DNS) which is time consuming and also costly at the same time. The neural network time series tool is used to validate the drag coefficients obtained by the simulation and was found acceptable as all the predicted value are within the acceptable error range.

VI. NOMINCLATURE

U	Average bulk velocity (m/s)
τ	Reynolds stress tensor
υ	Kinematic viscosity
ρ	Density of fluid
P	Pressure
υ_t	Turbulent viscosity
$\tilde{\upsilon}$	Working kinematic viscosity
K	Sub grid scale kinetic energy
τ_{ij}	Sub grid scale stress tensor
S_{ij}	Large scale stress tensor.
Δ	Grid spacing (m)
S_t	Strouhal number (Dimensionless)
F	Frequency (Hz)
Co	Courant number (Dimentionless)
N_{Re}	Reynolds number (Dimensionless)

REFERENCES

[1] Smagorinsky J., 1963' "*General Circulation experiments with the primitive equations*", Mon. Wea. Rev., 91,99-164.

[2] Spalart, P. R. and Allmaras, S. R., "*A One-Equation Turbulence Model for Aerodynamic Flows*," Recherche Aerospatiale, No. 1, 1994, pp. 5-21.

[3] Mohd. Ariff, Salim M. Salim and Siew Cheong Cheah, " *Wall y^+ approach for dealing with turbulent flow over a surface mounted cube : Part – I – Low Reynolds no.*" Seventh International conference on CFD in the minerals & process Industries, CSIRO, Melbourne, Australia, 9-11 Dec. 2009.

[4] Kolmogorov A. N. *The local structure of turbulence in incompressible viscous fluid for very large Reynolds numbers.Dokl. Akad*. Nauk., Vol. 30, pp. 301 – 305, 1941. Reprinted Proc. Royal Soc. London; 434; 9; 1991.

[5] Patankar, S. V. And Spalding, D.B., "*A Calculation Procedure for Heat Mass and Momentum Transfer in Three Dimensional Parabolic Flows*", Int. J. Heat and Mass Transfer, Vol 15, pp 1787-1805, 1972.

[6] Versteeg H K & Malalasekera W, *An Introduction to Computational Fluid Dynamics*, The Finite Volume Method: Longman Scientific & Technical, pp. 150-154, (1995).

[7] Prandtl L. Uber ein neues formelsystem fur die ausgebildete turbulenz *(On a new formation for the fully developed turbulence)*. Technical report, Academy of Sciences, 1945.

[8] Launder B.E. and Spalding D.B. *The numerical computation of turbulent flows*. Computer methods in applied mechanics and Engineering, Vol. 3, pp. 269–289, 1974.

[9] Hwang R.R. and Jaw S.-Y. *Second order closure turbulence models*, their achievements and limitations. Proc. Natl. Sci. Counc., Vol. 22, No. 6, pp. 703–722, 1998. ROC(A).

[10] Paik Joongcheol, Fotis Sotiropoulos, Fernando Porte – Agel, " *Detached eddy nsimulation of flow around two wall-mounted cubes in tandem*" International Journal of Heat and Fluid Flow, pp. 286 – 305, (2009).

[11] Matthew F. Barone, and Christopher J. Roy, "*Evaluation of Detached Eddy Simulation for Turbulent Wake Applications*" AIAA JOURNAL, Vol. 44, pp. 3062-3071, (12, December 2006).

[12] OpenFoam website: www.openfoam.org/docs/user/cavity.php#x5-120002.1.3

[13] Martinuzzi, R., Tropea, C., "*The flow around surface-mounted, prismatic obstacles placed in a fully developed channel flow*". Trans. ASME, J. Fluid Eng. 115 (1), 85–91 (1993).

[14] Meinders, E., Hanjalic´, "*Vortex structure and heat transfer in turbulent flow over a wall-mounted matrix of cubes. Int. J. Heat Fluid Flow*" 20, pp. 255–267 (1999)

[15] Meinders, E., Hanjalic´," *Experimental study of the convective heat transfer from in-line and staggered configurations of two wall mounted cubes*". Int. J. Heat Mass Transfer 45, 465–482. (2002).

[16] Meinders, E., van der Meer, T., Hanjalic´, K., "*Local convective heat transfer from an array of wall-mounted cubes*". Int. J. Heat Mass Transfer 41 (2), 335–346 (1998).

[17] Meinders, E., Hanjalic´, K., Martinuzzi, R., " *Experimental study of the local convection heat transfer from a wall-mounted cube in turbulent channel flow*" Trans. ASME, J. Heat Transfer 121, 564–573 (1999).

[18] Alexander Yakhot , Heping Liu , Nikolay Nikitin, "*Turbulent flow around a wall-mounted cube: A direct numerical simulation*" International Journal of Heat and Fluid Flow 27" pp. 994–1009 (2006).

[19] Thorsten Stoesser , Fabrice Mathey , Jochen Fröhlich 3, Wolfgang Rodi, "*Les Of Flow Over Multiple Cubes*" ERCOFTAC Bulletin, March 2003

[20] Breuer, M., Rodi, W. "*Large Eddy Simulation of Complex Turbulent Flows of Practical Interest. In: Notes on Numerical Fluid Mech., Flow Simulations with High Performance Computers II*." Ed.: Hirschel, E. H. Vieweg, Braunschweig. pp 258-274 (1996).

[21] Lodh Bibhab Kumar, Das Ajoy K, Singh N, "*Numerical Comparison Of Large Eddy Simulation Of Turbulence Modeling For Flow Past Wall Mounted Cubical Building Using Smagorinsky And Spalartallmarasddes Scheme*" Thirtieth National Convention and National Seminar on Recent Trends in Research, Development And Innovation In Chemical Industries" September' 2014.